Lawrence Berkeley Laboratory
UNIVERSITY OF CALIFORNIA

Presented at the Nordic Meeting on Nuclear Physics, Fuglsø, Denmark, August 16-20, 1982

PROPERTIES OF NUCLEI AT HIGH SPINS

F.S. Stephens

October 1982

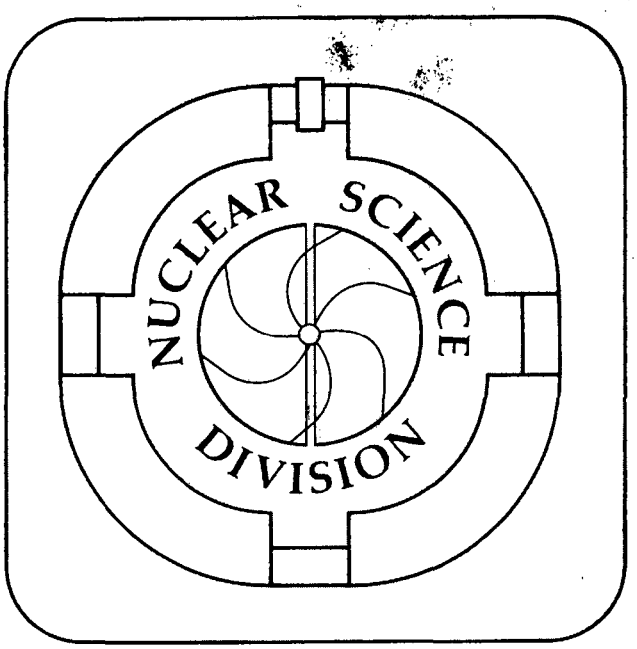

Prepared for the U.S. Department of Energy under Contract DE-AC03-76SF00098

DISCLAIMER

LBL-15070

Lawrence Berkeley Laboratory
University of California
Berkeley, California

PROPERTIES OF NUCLEI AT HIGH SPINS

F. S. Stephens

This work was supported by the Director, Office of Energy Research, Division of Nuclear Physics of the Office of High Energy and Nuclear Physics of the U. S. Department of Energy under Contract No. DE-AC03-76SF00098.

PROPERTIES OF NUCLEI AT HIGH SPINS

F. S. Stephens

Nuclear Science Division, Lawrence Berkeley Laboratory
University of California, Berkeley, CA 94720

Abstract: Nuclei generate high spins by two methods, alignment of single particle angular momentum and collective rotation. The competition of these two modes is discussed for the highest spins $40 \lesssim I \lesssim 65\hbar$. Evidence is presented that alignment of the $h_{9/2}$ and $i_{13/2}$ proton obitals from the next higher major shell produces large affects at high spins in rotational nuclei in the A = 160-166 region. It is suggested that such major shell effects produce the still larger irregularities known to occur in the lighter nuclei of this region.

1. Introduction

Nuclei can generate high angular momentum either by alignment along a common axis of the angular momentum of several individual nucleons or by a collective rotation of the nucleus as a whole. Recent developments in this field have been centered on understanding the competition of these two modes. This can be illustrated in fig. 1, where level schemes of ^{158}Er and ^{147}Gd are shown [1,2]. The ^{158}Er scheme is quite regular and the dominant behavior is collective rotation of a prolate-deformed nucleus as is illustrated at the left of fig. 1. The ^{147}Gd scheme is quite irregular, with complicated decay pathways and isomeric states (dark levels). Its dominant behavior is certainly single-particle alignment, as is illustrated at the right of fig. 1. Yet both of these schemes contain elements of the other type of behavior. There are irregularities in the ^{158}Er rotational pattern at spins around 16 and 26, which correspond to single particle alignments, and the 49/2+ isomer at 8.6 MeV in ^{147}Gd has a quadrupole moment that suggests that the aligned particles are polarizing the core so a collective oblate shape is developing. Below about I = 40$\hbar$, the γ-ray spectra from H.I.-fusion reactions contain resolved lines, and very detailed spectroscopic informaton on the levels can be obtained. Such data will be presented later in this meeting and I will not discuss them further here. Above about I $\approx$ 40$\hbar$ there are no resolved lines in the spectra and the information about the nuclear structure is less specific. It has generally been discussed in terms

of nuclear shapes and moments of inertia. The present discussion will be centered mainly on the latter of these two quantities.

2. Moments of Inertia

As a consequence of the interplay between collective and single particle motions, there are a variety of moments of inertia one can measure and compare with detailed nuclear-model calculations. The first distinction to make is between kinematic and dynamic values. The lowest order equation for rotational motion is the usual:

$$E = \frac{\hbar^2}{2\mathcal{J}} I(I+1) \approx \frac{\hbar^2}{2\mathcal{J}} I^2 \qquad (1)$$

where the one can generally be neglected compared with I for the spins we want to consider. A moment of inertia may be defined from the first derivative of this energy with respect to spin:

$$\frac{\mathcal{J}^{(1)}}{\hbar^2} = I\left(\frac{dE}{dI}\right)^{-1} = \frac{I}{\hbar\omega}\,, \qquad (2)$$

where $\mathcal{J}^{(1)}$ is called the "kinematic" moment of inertia because it has to do with the motion of the system--the ratio of angular momentum to angular frequency. It is also apparent that the second derivative leads to a definition:

$$\frac{\mathcal{J}^{(2)}}{\hbar^2} = \left(\frac{d^2E}{dI^2}\right)^{-1} = \frac{dI}{\hbar d\omega}\,, \qquad (3)$$

where $\mathcal{J}^{(2)}$ is called the "dynamic" moment of inertia since it has to do with the way the system will respond to a force. If there is only the kinetic energy term as given in eqn. 1, these are equal; but, in general, when there are additional I-dependent terms in the Hamilton-

ian these two moments of inertia will differ. In the present case, the Coriolis force perturbs the internal nuclear structure, giving rise, in lowest order, to an $(I \cdot j)$ term, so that $\mathcal{J}^{(1)} \neq \mathcal{J}^{(2)}$. This situation is not uncommon in other branches of physics. The arguments carry over into translational motion, where $p^2/2m$ is analogous to $I^2/2\mathcal{J}$, and additional momentum-dependent terms in the Hamiltonian give rise to two observed masses. Bohr and Mottelson have pointed out [3] that an electron moving in a crystal lattice is a close analog, where the kinematic mass determines the level density and related statistical mechanical properties; whereas the response of the electron to an external force depends on a different, dynamic mass.

These two moments of inertia can be defined in principle for any sequence of states desired, but certain ones occur rather naturally in the decay processes. So long as the particle configuration is frozen, so that one is confined to a band, the appropriate moments of inertia are $\mathcal{J}^{(1)}_{\text{band}}$ and $\mathcal{J}^{(2)}_{\text{band}}$. If there is no perturbatin (alignment, shape change, etc.) of the internal structure along this band, these correspond to "collective" values, and this is an approximation I will often use. In general, however, a single decay pathway involves a sequence of bands having different alignments. Then the overall variation of spin with frequency is different and defines "effective" moment of inertia $\mathcal{J}^{(1)}_{\text{eff}}$ and $\mathcal{J}^{(2)}_{\text{eff}}$. This $\mathcal{J}^{(2)}_{\text{eff}}$ is a slightly different moments of inertia than has been previously defined, but seems to be an appropriate one, both experimentally and theoretically. It is defined for any frequency and, in regions of backbends, a given fre-

quency contains contributions from both bands, giving rise to very high values. There are several reasons for preferring this $\mathcal{J}^{(2)}_{eff}$: 1) it is easy to measure experimentally as will be shown; 2) it can be measured with high resolution (small ω intervals) giving more detailed information; 3) its integral gives the usual $\mathcal{J}^{(1)}_{eff}$; and 4) the mathematical relationships we want to use require an $\mathcal{J}^{(2)}$ that is the <u>total</u> spin change in a frequency interval. The last point has to do with separating the spin increment ΔI into a part within the band ΔI_b (mostly collective) and an alignment Δi. Defining $\mathcal{J}^{(2)}_{eff}$ as the <u>total</u> spin change, $\Delta I/\Delta\omega$, leads to:

$$\frac{\Delta i}{\Delta I} = 1 - \frac{\mathcal{J}^{(2)}_{band}}{\mathcal{J}^{(2)}_{eff}} \quad . \tag{4}$$

For the unresolved spectra from the highest spin states, the population is spread over many bands in many decay sequences. Nevertheless, the average band moments of inertia can be determined by looking for successive rotational transitions as correlations in γ-γ coincidence spectra. Similarly, the overall spin and γ-ray energies and their variations are also measurable giving the average effective moments of inertia. Thus we can obtain information about Δi in these regions.

3. Experimental Data on Moments of Inertia

A number of studies have been made over the last 10-15 years of the unresolved γ rays emitted from the highest spin states. It has been established that there are two types of γ rays emitted: statistical ones (3 or 4) that cool the nucleus to the yrast line and "yrast-like" ones ($\gtrsim 25$) that remove the angular momentum and contain

most of the nuclear structure information. For some nuclei essentially all the yrast-like transitions are collective rotational ones, and for most nuclei at least those from the very highest spin states are. In addition, systematic searches for noncollective behavior (as evidenced by the existence of isomers) have given negative results, generally above ~30ħ, and in all cases surveyed above 40ħ. Thus the methods developed to study the highest spin states center on ways to extract information from unresolved rotational sequences and use the moment of inertia concepts discussed above.

3.1. Measurement of $\mathcal{J}^{(2)}_{band}$

The γ-ray spectrum from a rotational nucleus is highly correlated in time, spatial distribution, and energy. For a perfect rotor, it is easy to show from eqn. 1:

$$E_\gamma = 2\frac{dE}{dI} = \frac{\hbar^2}{2\mathcal{J}}(4I_i - 2) , \qquad (5)$$

where I_i is the initial spin. This spectrum is composed of equally spaced lines, up to some maximum energy corresponding to the decay of the state with highest angular momentum, I_{max}. One aspect of the energy correlations is that no two γ rays have the same energy. If plotted on a two-dimensional diagram of $E^{(1)}_\gamma$ vs $E^{(2)}_\gamma$, such energies give a pattern with no points along the diagonal and a series of ridges parallel to it. The width of the "valley" W along the diagonal is determined by the difference between γ-ray energies and is thus related to the band moment of inertia,

$$W = 2\Delta E = 4\frac{dE_\gamma}{dI} = i\frac{d\omega}{dI} = \frac{8\hbar^2}{\mathcal{J}^{(2)}_{band}} . \qquad (6)$$

The important point is that the spectrum need not be resolved to determine the valley width. All that is required is that the populated bands have somewhat similar moments of inertia at a given frequency (γ-ray energy).

The data [4] in fig. 2 come mainly from ^{159,160}Er nuclei formed by bombarding ^{124}Sn with ^{40}Ar at sufficient energy (184 MeV) to bring into the fused system all the angular momentum the nucleus can hold ($\sim 70\hbar$). The data have been "symmetrized" around the diagonal in order to improve the statistics and have an "uncorrelated" background subtracted. A valley is clear up to energies ~ 1 MeV, and again probably from 1.1 to 1.2 MeV. Resolved lines have been seen in this case only up to $\sim$ 0.8 MeV. The width of the valley in both the upper and lower region is about the same and can be evaluated to give $\mathcal{J}^{(2)}_{band}/\hbar^2 \approx 50$ MeV^{-1}, around two-thirds of the rigid-body value.

In these correlation plots, the valley can be filled by irregularities in the bands, alignments, for example. These produce several transitions in the same energy region, and not only fill the valley but produce "stripes" of higher coincidence intensity at these γ-ray energies [5]. It is important to appreciate that the alignments are expected to occur in many bands at nearly the same frequency since the alignment of a given pair of nucleons should depend only weakly on the rest of the configuration. These correlation techniques are potentially powerful, but not so much information has yet come from them. One problem has to do with statistics--for a pair of Ge detectors with

peak-to-total areas of 0.15, the fraction of good coincidence events (full energy-full energy) is only ~2%. Furthermore, the analysis techniques are still developing, so that one is not yet quite sure which features of the data can be fully trusted. It is my opinion that this method will only reach its full potential when the analysis methods are better understood and arrays of Compton-suppressed Ge detectors are used. Rather rapid progress is being made in both these areas.

3.2. Measurement of $\mathcal{J}^{(2)}_{eff}$

The effective moments of inertia are simpler in some respects. They involve only relating a collective γ-ray energy with a spin or measuring the number of γ rays in an energy interval. The former gives $\mathcal{J}^{(1)}_{eff}$ values and has been measured several different ways, originally by relating the maximum γ-ray energy in a spectrum with the estimated maximum spin input. Recently, however, reliable methods for obtaining $\mathcal{J}^{(2)}_{eff}$ have been developed [6] and these are much more sensitive to the nuclear structure. If desired $\mathcal{J}^{(1)}_{eff}$ can then be obtained by integration. It is apparent that in a spectrum consisting only of "stretched" electric quadrupole ($I \rightarrow I-2$) transitions (which is known to be a good approximaton in regions of rotational behavior), the number of transitions dN in a given γ-ray energy interval is just half the spin removed from that interval. If one knows the fraction of the observed population that goes through the interval, $f(E_\gamma)$, then (remembering $E_\gamma = 2\hbar\omega$):

$$\frac{H(E_\gamma)}{f(E_\gamma)} = \frac{dN}{dE_\gamma} = \frac{dI}{4\hbar d\omega} = \mathcal{J}^{(2)}_{eff}(\omega)/4\hbar^2 \ . \qquad (7)$$

The height of the spectrum $H(E_\gamma)$ gives directly $\mathcal{J}^{(2)}_{eff}(\omega)$. This was long recognized, but the difficulty was to find the feeding, $f(E_\gamma)$. Recently a method was developed [7] using the spectra from two similar but slightly shifted spin distributions, whose difference is generally proportional to the feeding curve. For a constant spin shift ΔI, one can show:

$$H(E_\gamma) - H_\Delta(E_\gamma) = \Delta I \frac{df(E_\gamma)}{dE_\gamma} \ , \qquad (8)$$

so that:

$$f(E_\gamma) = \int_{E_\gamma}^{\infty} \frac{df(E_\gamma)}{dE_\gamma} dE_\gamma \Big/ \int_0^{\infty} \frac{df(E_\gamma)}{dE_\gamma} dE_\gamma \ . \qquad (9)$$

4. Results

4.1. Rotational Nuclei: A = 160-166

Figure 3 shows a spectrum of ^{159,160}Er resulting from the decay of a rather broad spin distribution centered at ~55ħ. (This distribution is defined by selecting coincidences with a slice of the total γ-ray energy emitted by the nucleus. The total energy is detected in a large NaI crystal having an overall solid angle times efficiency of ~0.75 of 4π.) The statistical spectrum of γ rays, whose high-energy tail is seen above ~2 MeV, is subtracted leaving a spectrum of essentially pure collective transitions, and the $\mathcal{J}^{(2)}_{eff}$

values shown by the solid line in fig. 4 result from correcting this for feeding [7]. Two other cases, ^{161,162}Yb and ^{165,166}Yb, are also shown in fig. 4. The general rise at low frequencies in all these nuclei is due to the quenching of the pairing correlations, and the irregularities below $\hbar\omega \sim 0.3$ MeV result from both the partially resolved individual γ-ray transitions and the known alignments (backbends), which cause several transitions to pile up at the same frequency. The band moments of inertia from the correlation data are plotted as lighter lines in the regions where they have been determined. The rise in the effective moments of inertia above frequencies of 0.5 MeV seem to be associated with a drop in the band values. This suggests that alignments are becoming more important contributors of angular momentum. The higher values for the Yb (Z = 70) nuclei compared with ^{159,160}Er (Z = 68) suggests that protons play an important role here, which is in accord with calculations [8] that predict proton $h_{9/2}$ and $i_{13/2}$ alignments in this frequency region. Thus the rise is due to levels dropping down from the next higher major shell and constitutes the first evidence for such levels as large contributors to the angular momentum. According to general arguments an increase in aligned, relative to collective, angular momentum could indicate a shift away from $\gamma = 0°$ into the triaxial region, but such conclusions about the nuclear shape are rather speculative.

It is somewhat puzzling that these $\mathcal{J}^{(2)}_{\text{eff}}$ values do not show any detailed structure at the highest frequencies. An interesting explanation could be that there are essentially no conserved quantum numbers at these frequencies, and all bands behave similarly. But this seems

unlikely, both from theoretical grounds and from the absence of highly correlated γ-ray spectra (well-developed valley-ridge structure) that should result. More likely the irregularities are washed out because the observed population is spread over many configurations and a broad temperature region. Restricting these population spreads should then reveal a wealth of detailed information. There is great hope that the 4π NaI "balls" that now exist may restrict the population sufficiently to resolve many more lines. We will hear reports from these crystal balls later in this meeting.

4.2. Transitional Nuclei: $A \approx 150$-166

In the previous section it was observed that levels from the next higher major shell ($h_{9/12}$ and $i_{13/2}$ protons) can contribute rather large amounts of angular momentum to the system at sufficiently high frequencies ($\hbar\omega \approx 0.5$-0.6 MeV). We believe there is evidence that such shell effects play an even larger role in the lighter nuclei of this region [9]. Figure 5 shows the spectra from two Er systems taken several years ago [10]. The heavier system leads mainly to the rotational nucleus ^{160}Er, and its spectrum is smooth, as might be expected for a good rotor, except for a peak at $\hbar\omega \approx 0.3$ MeV caused by the first backbend. The lighter system leads mainly to ^{155}Er, a nucleus that is between the region of rotational and non-rotational nuclei. In this system one sees two large peaks, one at frequencies below ~0.5 MeV, and the other centered around frequency ~0.65 MeV. It is known that in ^{156}Er and ^{158}Er the lower peak is composed mostly of collective E2 transitions, and that all three major alignments of

the valence shell of nucleons (ν, $i_{13/2}$; π, $h_{11/2}$; and ν, $h_{9/2}$) occur in this lower frequency region. In ^{154}Er the lower peak is quite different in composition, though very similar in appearance. It is composed of about half dipole and half quadrupole transitions, and the structure of both ^{154}Er and ^{162}Dy is known to be mainly non-collective, but again made up out of the valence shell of nucleons. Thus, by about spin 40$\hbar$ in the A $\approx$150-160 region one has used up all the major alignments of the valence shells and generation of angular momentum from these shells of nucleons must become more difficult, leading to small moments of inertia. This, we propose, causes the lower bump to drop sharply around 1 MeV, and the height of the spectrum (proportional to $\mathcal{J}^{(2)}_{eff}$) would remain low if only valence nucleons were considered.

The second peak in all the Er (and adjacent) nuclei is composed of stretched E2 transitions (presumably collective), and looks very much like the upper part of the smooth spectrum in the heavier rotational nuclei. To be such a large peak in these spectra (see fig. 5) it must represent a new source of angular momentum, and that source is very likely the next major proton shell, where π, $i_{13/2}$ and π, $h_{9/2}$ would be the first contributors, just as found for the heavier rotational nuclei. There are probably also shape changes associated with at least some of these alignments, since the upper bump of all the Er nuclei seems similar, whereas the lower bump is non-collective for the lighter systems, but collective for the heavier ones. The data are consistent with triaxial shapes and

modest deformations ($\varepsilon \sim 0.3$) for these highest-spin regions, but there is little direct evidence for such shapes.

One of the main points here is that some properties, like shape, may be rather difficult to determine with confidence for these regions, whereas others, like the major shell effects, can sometimes be almost directly observable as broad peaks in the spectra. The lower peak occurs in the 150-156 mass region for the Er nuclei because the Fermi level is in the right place (low) for alignments here, and the deformation is not well stablized, leading to valence shell alignments at very low frequencies. In the heavier systems $A \gtrsim 160$, the axially symmetric prolate deformation is very stable, and the Fermi level begins to be too high for easy alignment, both of which spread the valence shell contributions up to higher frequencies and thus destroy the two-peak structure.

5. Conclusion

The study of moments-of-inertia can give considerable insight into the physics of rotating nuclei even if the spectra are not resolvable. We have shown how the measurement of $\mathcal{J}^{(2)}_{band}$ and $\mathcal{J}^{(2)}_{eff}$ can give an indication of the amount of aligned vs. rotational angular momentum in a given spin interval. Such analyses on the good rotational nuclei of the $A \approx 160$-166 region suggest that there are major alignments coming from the next major shell (proton $i_{13/2}$ and $h_{9/2}$) in the frequency region above ~0.6 MeV. This has led us to speculate that such major shell effects may be responsible for the well known two-peak structure in the spectra of the lighter Er and Dy nuclei.

These moment-of-inertia analyses are somewhat qualitative, and certainly much less informative than the detailed spectroscopic studies made on the resolved spectra of nuclei below ~35ħ. It seems possible that the new 4π detector systems will enable us to resolve the spectra up to 60-70ħ, the full region populated, which would would give enormously more detailed information at the highest spins. However, if that proves not to be the case then these moment-of-inertia techniques will probably be our best source of information on nuclear structure at the highest spins, and it is becoming apparent that they can give considerable information.

This work was supported by the Director, Office of Energy Reserach, Division of Nuclear Physics of the Office of High Energy and Nuclear Physics of the U. S. Department of Energy under Contract No. DE-AC03-76SF00098.

References

1. Burde, J., Dines, E. L., Shih, S., Diamond, R. M., Draper, J. E., Lindenberger, K. H., Schuck, C. and Stephens, F. S., Phys. Rev. Lett. 48 530 (1982).

2. Hausser, O., Mahnke, H.-E., Sharpey-Schafer, J. F., Swanson, M. C., Taras, P., Ward, D., Andrews, H. R. and Alexander, T. K., Phys. Rev. Lett 44 132 (1980): Bakander, O., Baktash, C., Borggreen, J., Jensen, J. B., Kownacki, J., Pedersen, J., Sletten, G., Ward, D., Andrews, H. R., Hausser, O., Skensved, P. and Taras, P., preprint (1982).

3. Bohr, A. Mottelson, B. R., Physica Scripta 24, 71 (1981).

4. Deleplanque, M. A., Stephens, F. S., Andersen, O., Ellegaard, C., Garrett, J. D., Herskind, B., Fossan, D., Neiman, M., Roulet, C., Hillis, D. C., Kluge, H., Diamond, R. M. and Simon, R. S., Phys. Rev. Lett. 45, 172 (1980).

5. Ellegaard, C., Deleplanque, M. A., Andersen, O., Herskind, B., Stephens, F. S., Diamond, R. M., Kluge, H., Schuck, C., Shih, S. and Draper, J. E., Phys. Rev. Lett. 48, 670 (1982).

6. Simons, R. S., Banaschik, M. V., Diamond, R. M., Newton, J. O. and Stephens, F. S., Nucl. Phys. A290, 253 (1977).

7. Deleplanque, M. A., Korner, H. J., Kluge, H., Macchiavelli, A. O., Bendjaballah, N., Diamond, R. M. Stephens, F. S., submitted to Phys. Rev. Lett.

8. Bengtsson, T. and Ragnarsson, I, preprint, 1982.

9. Deleplanque, M. A., Diamond, R. M., Dines, E. L., Draper, J. E., Macchiavelli, A. O. and Stephens, F. S., to be published.

10. Deleplanque, M. A., Husson, J. P., Perrin, N., Stephens, F. S., Bastin, G., Schuck, C., Thibaud, J. P., Hildingsson, L., Hjorth, S., Johnson, A. and Lindblad, Th., Phys. Rev. Lett. 43, 1001 (1979).

Figure Captions

Fig. 1. Level scheme for ^{158}Er and ^{147}Gd, together with illustrations of the dominant source of angular momentum for each case.

Fig. 2. Correlation spectrum from the reaction $^{124}Sn(^{40}Ar,xn)^{164-x}Er$ at 185 MeV. The data were taken on GeLi detectors and treated according to ref. 4. The plot shows contours of equal numbers of correlated events, where the darker regions have more counts according to the scale at the right edge.

Fig. 3. Unresolved γ-ray spectrum for the indicated reaction taken with a NaI crystal and corrected for response function. The spectrum is that in coincidence with a slice of high-energy events (implying high spin) recorded in a large total-energy γ-ray detector.

Fig. 4. $\mathcal{J}^{(2)}_{eff}$ as a function of $\hbar\omega$ for the systems $^{124}Sn + ^{40}Ar$ (thick solid line), $^{126}Te + ^{40}Ar$ (dotted line), and $^{130}Te + ^{40}Ar$ (thick dashed line). Also shown are some values of $\mathcal{J}^{(2)}_{band}$ for $^{124}Sn + ^{40}Ar$ (thin solid lines) and $^{130}Te + ^{40}Ar$ (thin dashed lines).

Fig. 5. Unresolved γ-ray spectra from targets of ^{119}Sn (left) and ^{124}Sn (right) bombarded with ^{40}Ar projectiles.

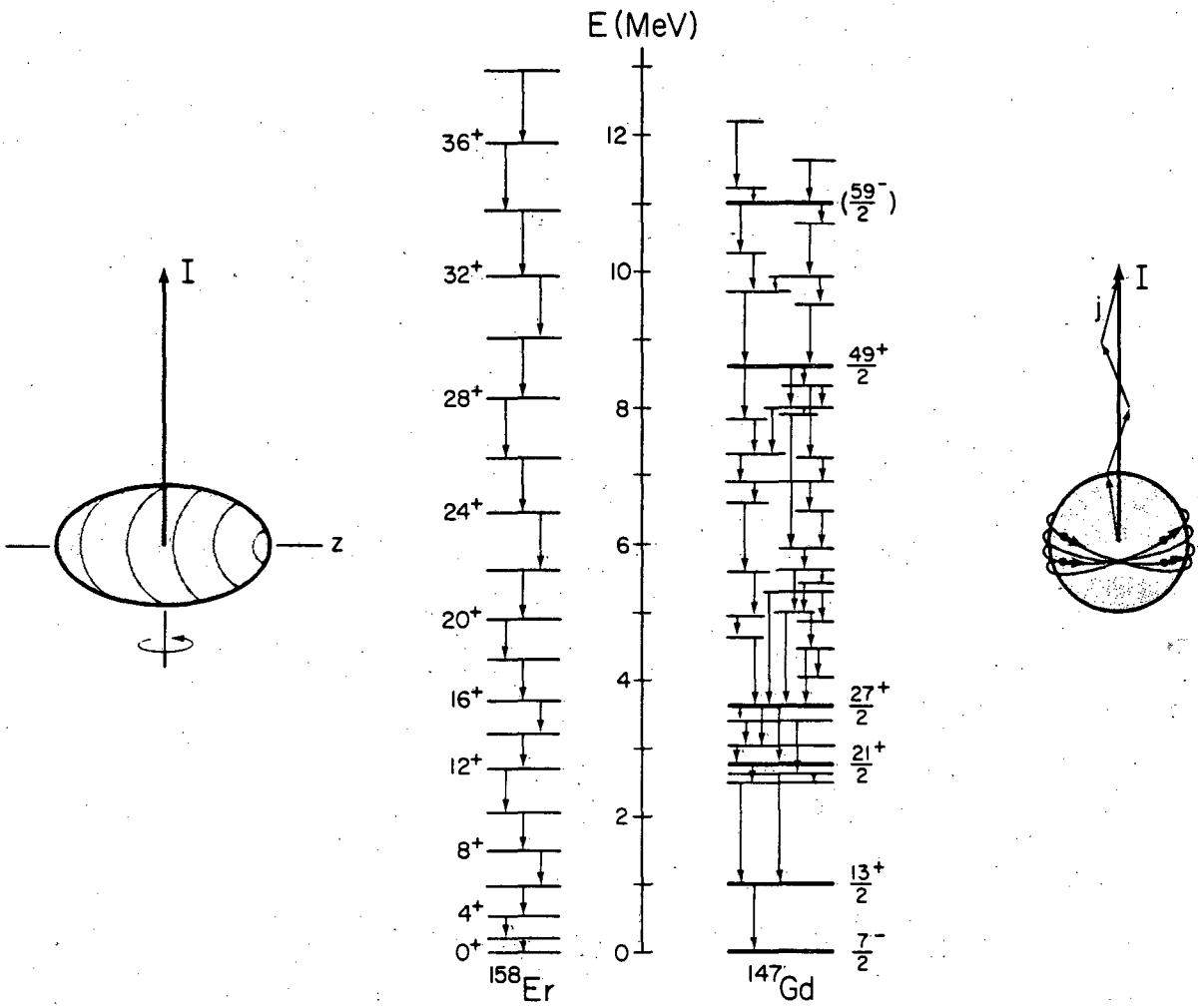

Fig. 1

XBL 828-1011

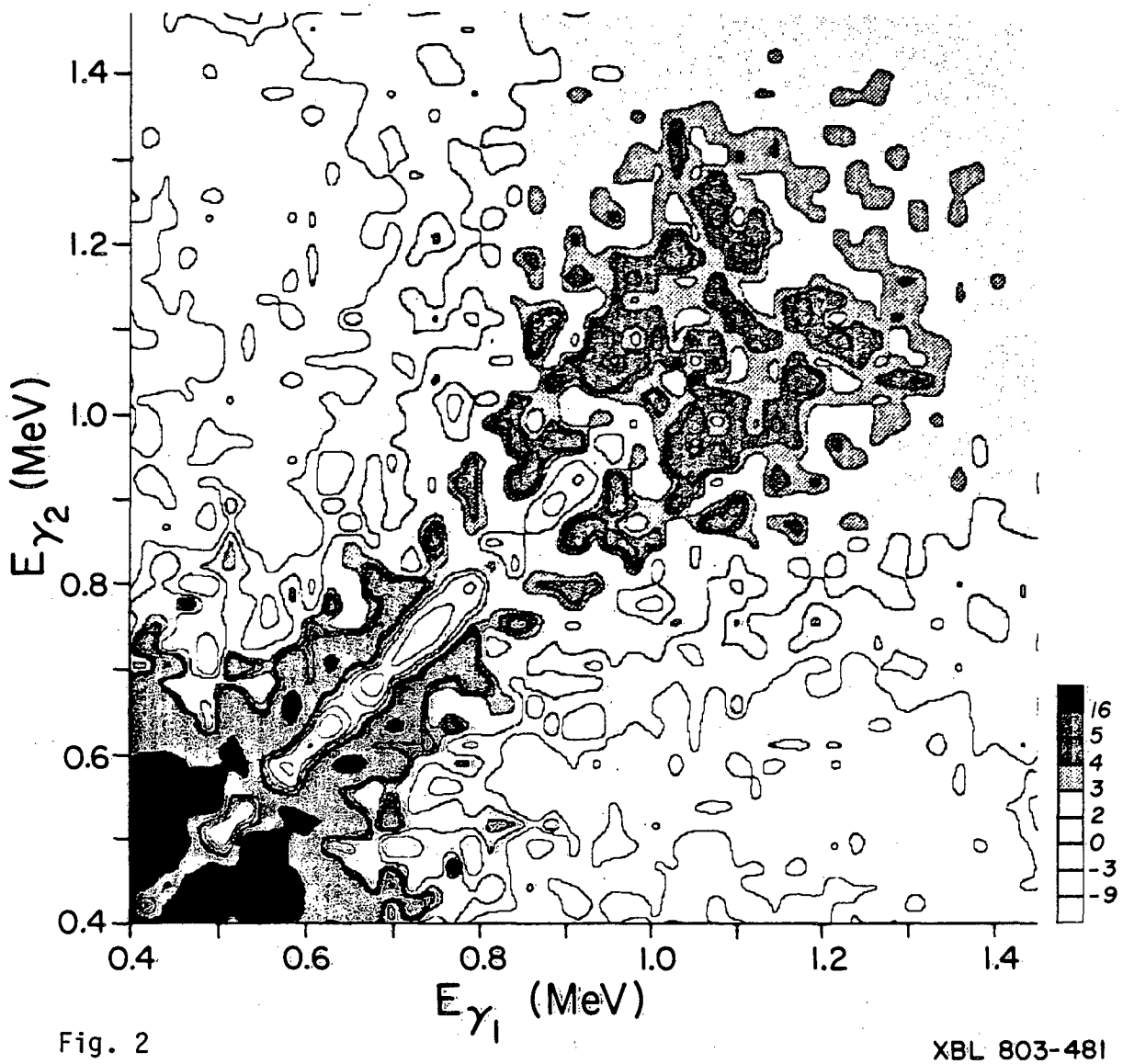

Fig. 2

XBL 803-481

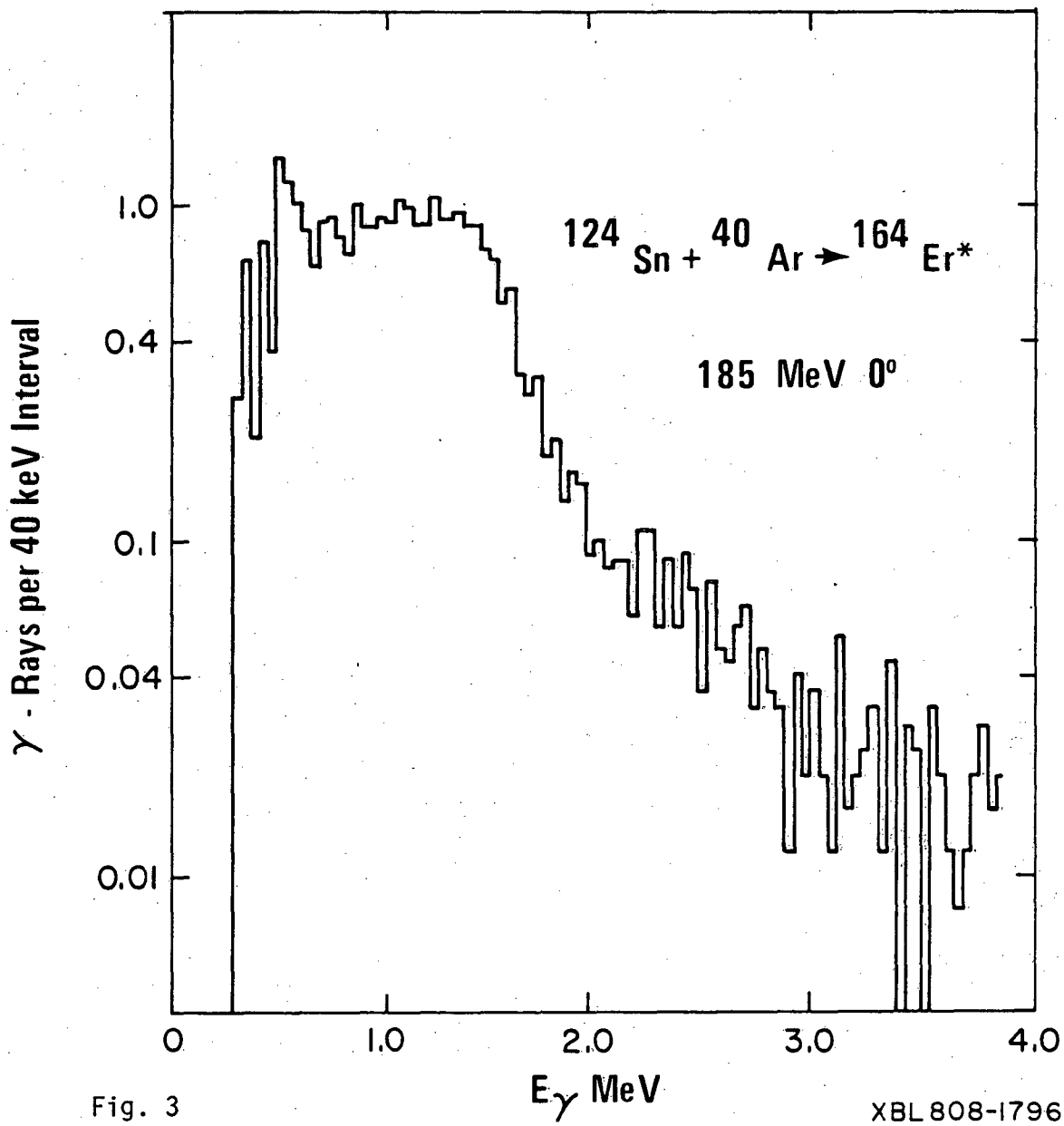

Fig. 3

XBL 808-1796

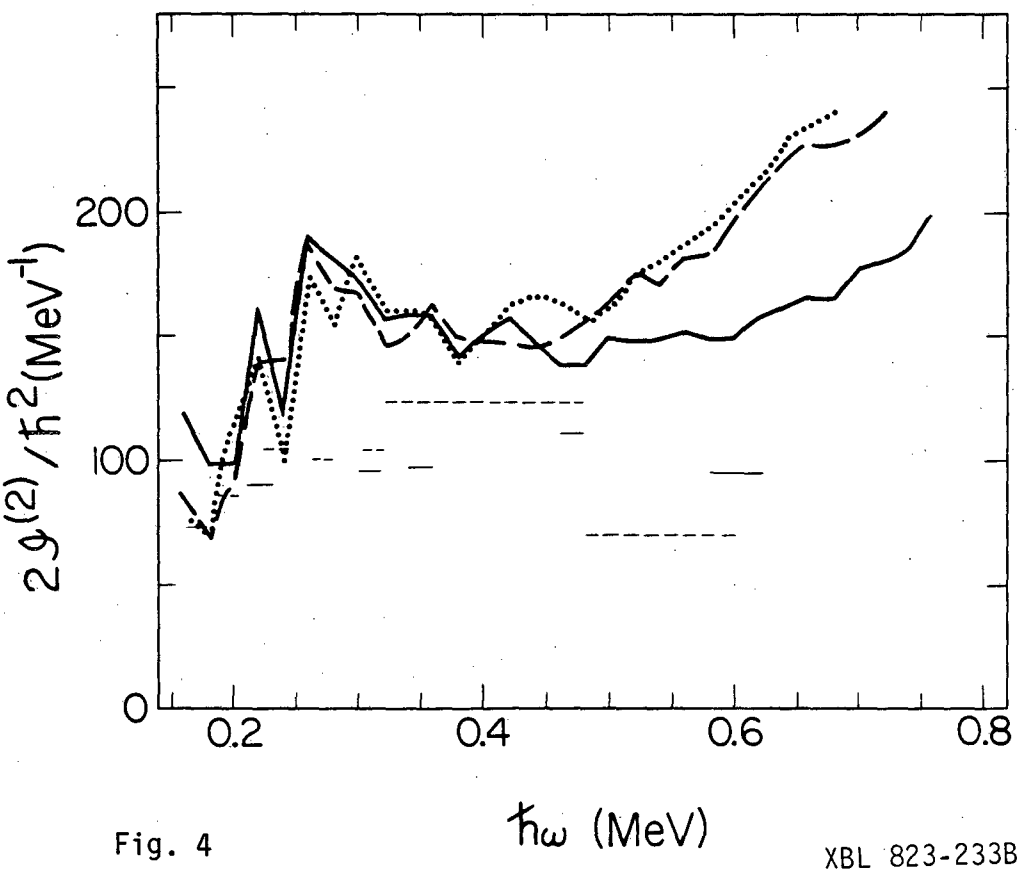

Fig. 4

XBL 823-233B

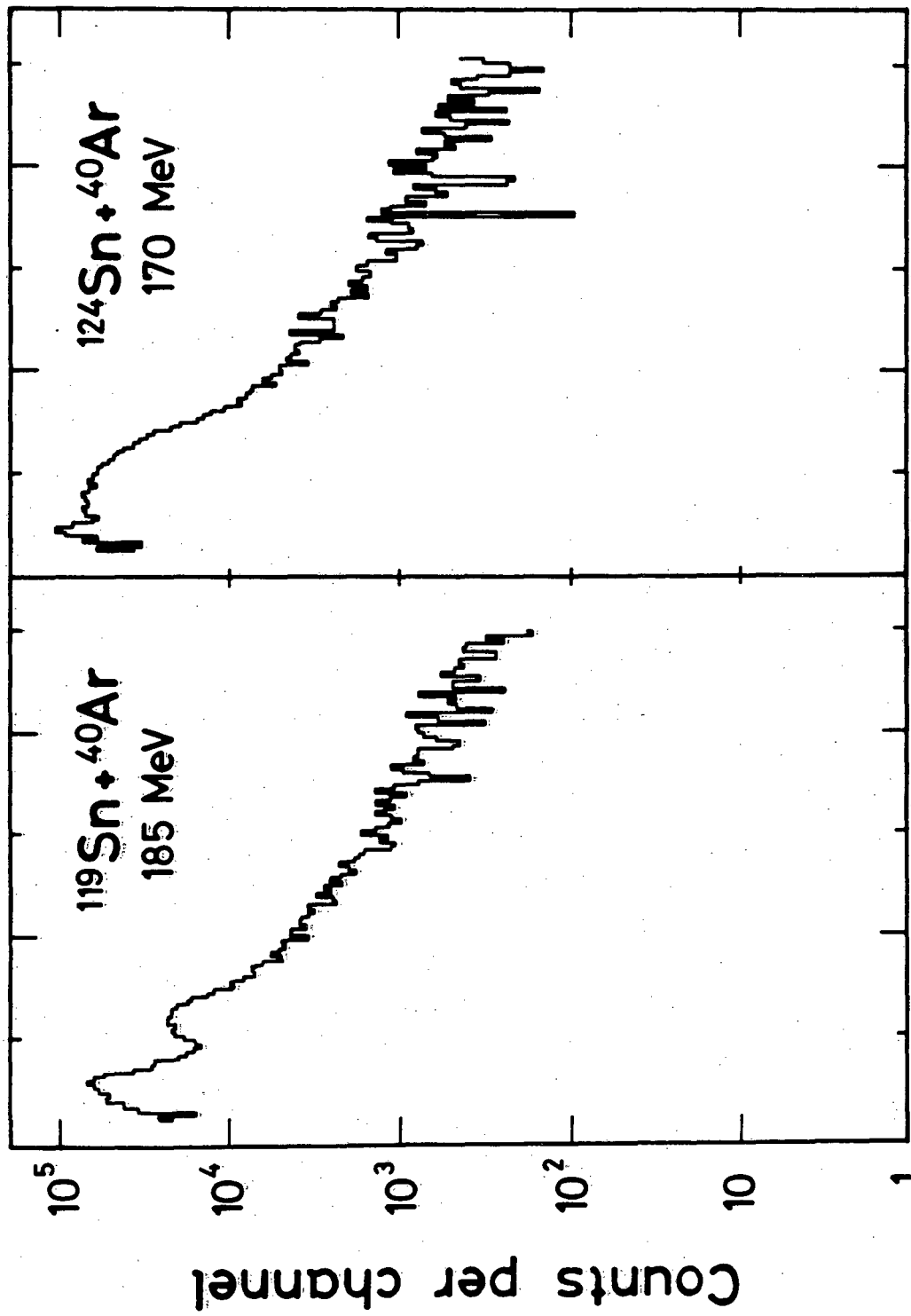

XBL 803-8761

Fig. 5

TECHNICAL INFORMATION DEPARTMENT
LAWRENCE BERKELEY LABORATORY
UNIVERSITY OF CALIFORNIA
BERKELEY, CALIFORNIA 94720